Investigation of a Novel Optical Phase Demodulator Based on a Sampling Phase-Locked Loop

Darko Zibar, Leif A. Johansson, Hsu-Feng Chou, Anand Ramaswamy, Mark Rodwell, John Bowers

Department of Electrical and Computer Engineering, University of California, Santa Barbara, CA 93106, USA, dz@ece.ucsb.edu

***Abstract* — A novel phase-locked coherent demodulator, based on a sampling phase-locked loop, is presented and investigated theoretically. The demodulator is capable of operating at high-frequencies, by using optical sampling to downconvert the high-frequency input RF signal to the frequency range of the baseband loop. We develop a detailed theoretical model of the (sampling) phase-locked coherent demodulator and perform detailed numerical simulations. The simulation results show that the operation of the sampling demodulator resembles the operation of the baseband demodulator for very short optical pulses (< 2 ps). Furthermore, the model is shown to be in good agreement with experimental results.**

***Index Terms* — analog links, microwave photonics, modulators, phase-modulation, sampling, PLL, coherent**

I. INTRODUCTION

The use of optical links for the transmission of RF signals is a subject of considerable interest for future commercial and military systems [1]. Intensity modulated analog optical links have long been limited by the nonlinear response of optical modulators [1]. The underlying reason for this is that the response of optical intensity modulators is "hard-limited" by zero and full transmission. In contrast, optical phase modulation has no fundamental limit to modulation depth besides that given by the available modulation range in optical phase modulators. The challenge to implement a linear phase modulated link lies in the receiver structure [2]. The traditional coherent receiver has sinusoidal response limiting the overall dynamic range. We have recently proposed, theoretically investigated and experimentally demonstrated a novel coherent optical phase-locked demodulator with feedback [3]-[4], resulting in 15 dB of SFDR improvement compared to the traditional approach. To overcome the nonlinearity issue of the traditional receiver, the local oscillator phase is locked to a received optical phase modulation using the feedback. The net input signal-LO phase difference is thereby kept sufficiently small to fall within the linear range of the receiver. In this paper, we show that there is a good agreement between the experimental and calculated results of the baseband (operation frequency: 0-2 GHz) demodulator. However, in order to operate the phase demodulator at high frequencies (>2GHz) than the base-band loop bandwidth would need to be very large to obtain a high degree of linearity. For instance a loop operating at 20 GHz would require >100GHz of loop bandwidth. This is far beyond feasible, considering the delay in the feedback loop. To overcome this problem, a novel approach using optical sampling at the demodulator is investigated. The basic idea is to use a pulsed laser source at the receiver unit, see Figure 1. The received high-frequency input RF signal is hence sampled at a rate close to the pulsed laser source period. In this way, an Intermediate Frequency, IF, component is obtained that falls within the operating range of the baseband optical phase-demodulator. Using a detailed numerical model, we investigate how the signal-to-intermodulation ratio of the demodulated optical signal is affected by the laser signal pulse width, loop gain, loop time-delay and input RF signal frequency. The dynamical behavior of the sampling loop is compared to that of the baseband loop.

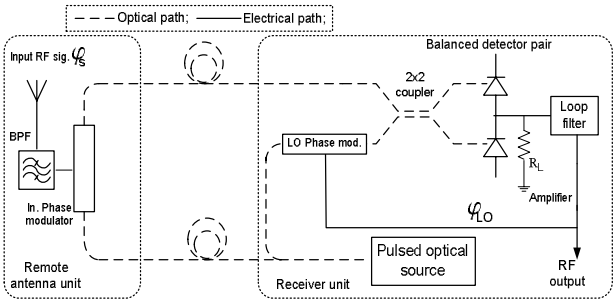

Fig. 1. General outline of phase modulated optical link and phase-locked optical demodulator at the receiver unit.

II. THEORY

The set-up of the optical phase demodulator, using a sampling phase-locked loop, on which we base our model, is shown in Fig. 1. The received RF signal, $\varphi_s(t)$, is used to directly modulate an input optical phase modulator at the remote antenna unit. The optical signal is then transported to the receiver unit where the optical signal phase, $\varphi_s(t)$, is compared to the reference phase (signal), $\varphi_{LO}(t)$, using the balanced detector pair with load resistance R_L. A single pulsed optical source is used for both the remote and the receiver unit. The signal from

the balanced detector pair, containing the phase difference between $\varphi_s(t)$ and $\varphi_{LO}(t)$, is then passed through the loop filter (low pass), amplified and applied to the LO phase-modulator. The original input RF signal, $\varphi_s(t)$, is now therefore downconverted to an IF: $\omega_{IF}=\omega_1-\omega_{ls}$. ω_1 is the frequency of the RF input signal and ω_{ls} is the repetition frequency of the pulsed optical source time-varying amplitude. The desired demodulated signal, $V_{out}(t)$, is the electrical signal tapped before the LO phase-modulator. In order to characterize the Spurious Free Dynamic Range (SFDR) of the system, the input RF signal is assumed to consist of two tones: ω_1 and ω_2. The dynamical behavior of the loop is fully determined by the total phase error defined as: $\phi_e(t)=\varphi_s(t)-\varphi_{LO}(t)$.The differential equation describing the total phase error in the loop becomes:

$$\frac{d\phi_e}{dt}=-\frac{\pi\omega_1 V_1^s}{V_{\pi,in}}\sin(\omega_1 t)-\frac{\pi\omega_2 V_2^s}{V_{\pi,in}}\sin(\omega_2 t)-K\sin[(\phi_e(t)]$$
$$+\frac{\pi A}{\tau_{LF}V_{\pi,LO}}V_{out}(t)-2c_2V_{out}(t)\left(K\sin[\phi_e(t)]-\frac{\pi A}{\tau_{LF}V_{\pi,LO}}V_{out}(t)\right)$$
$$-3c_3V^2{}_{out}(t)\left(K\sin[\phi_e(t)]-\frac{\pi A}{\tau_{LF}V_{\pi,LO}}V_{out}(t)\right) \qquad (1)$$

$Q=\pi A^2{}_{ls}(t)AR_{pd}R_L/V_\pi\tau_{LF}$. $A_{ls}(t)$ is the time-varying amplitude (i.e. Gaussian pulse train) of the pulsed optical source, A is the gain of the loop filter, R_{pd} is the responsivity of the photodiodes, R_L is the load resistance and τ_{LF} is inversely proportional to the BW of the loop filter. V^s_1 and V^s_2: are the amplitudes of the received input signal. $V_{\pi,in}$ and $V_{\pi,LO}$ are the voltages (assumed equal) of the input and LO phase-modulator in order to obtain π phase shift. c_1, c_2 and c_3 represent the terms of the polynomial expansion of the LO phase modulator response. The loop gain, K, is defined as: $K=\pi P^{av}{}_{ls}AR_{pd}R_L/V_\pi\tau_{LF}$, where $P^{av}{}_{ls}$ is the average power of the pulsed optical source. The nonlinear response of the phase detector, pulsed optical source, etc. will result in intermodulation distortion of the demodulated signal. 3rd order intermodulation products are especially important because they may set the Spurious Free Dynamic Range (SFDR) of the system [3]. The demodulated signal obtained by the sampling phase-locked optical demodulator is then characterized by the Signal-to-Intermodulation Ratio (SIR) which is the ratio between the power of the demodulated signal and the 3rd order mixing product.

When the loop is locked, the total phase error, for the baseband loop (CW optical source) is obtained by solving (1). For simplicity, we do not consider the loop filter, tracking phase-modulator nonlinearities are set to zero and the phase detection process is linear: $\sin[\phi_e(t)]\approx\phi_e(t)$. In order to avoid bulky expressions, we assume that the RF input signal consists of only one tone at frequency ω_1. For the baseband loop, the total phase error, $\phi_e(t)$, becomes:

$$\phi_e(t)=\frac{1}{K^2+\omega_1^2}\left(M_{in}\omega_1^2\cos(\omega_1 t)-K\sin(\omega_1 t)\right) \qquad (2)$$

where $M_{in}=\pi V^s_1/V_{\pi,in}=\pi V^s_2/V_{\pi,in}$. Since there are no non-linearities in the loop, $\phi_e(t)$ contains only a frequency component at ω_1, as expected. Equation (2) also shows that as K approaches infinity, $\phi_e(t)$ approaches zero. For the sampling loop, the solution of (1) is the same as the solution in (2), under the assumption that the pulse width of the laser is infinitely narrow ($A_{ls}(t)$ consists of delta functions). This means that for infinitely small laser signal pulse widths, the dynamics of the sampled loop will be the same as dynamics of the baseband loop. For a raised cosine pulse shape, the solution of (1) becomes:

$$\phi_e(t)=M_{in}\left(\cos[\omega_1 t]+\frac{A_0K\sin^3[\omega_1 t]}{6\omega_1}+\frac{A_0K\sin[\omega_1 t]-\omega_1 t\cos[\omega_1 t]}{2\omega_1}\right)$$
$$\times\exp\left(\frac{-0.5A_0K(\cos[\omega_1 t]\sin[\omega_1 t]+0.5\omega_1 t)}{\omega_1}\right) \qquad (3)$$

where A_0 is the amplitude of the pulses. It is observed in (3), that $\phi_e(t)$ not only contains the frequency components at ω_1, but also the multiples of ω_1 (harmonics). Equation (3) therefore indicates that the sampling will induce nonlinearities in the overall loop response. The amplitude of harmonics increases as the loop gain is increased. This is contrarst with the baseband loop. Furthermore, by inspecting (3), we can qualitatively conclude that the amplitude of the harmonics can be reduced by increasing the frequency ω_1. For the zero loop gain, (3) equals (2). In section IV, it is confirmed that the sampling induces extra nonlinearities in the overall loop response, by numerically solving the exact form of (1).

III. Baseband Experimental Results

The experimental set-up, similar to Fig. 1, was constructed in order to verify the (baseband) model [4]. A CW laser source is used in the experimental set-up.

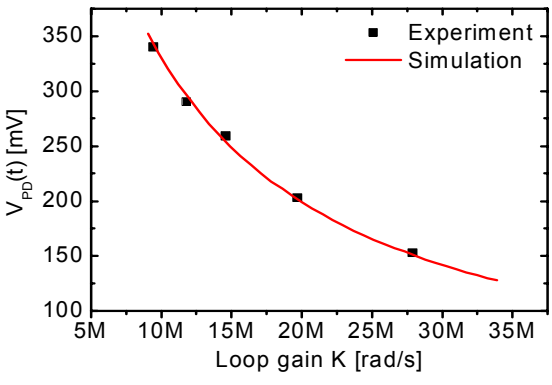

Fig. 2. One tone measurement. Output of the balanced photo-detector, $V_{pd}(t)$, as a function of loop gain.

In Fig. 2, a one-tone measurement is shown together with simulation results. The input RF signal frequency is f_1=150 kHz and the loop filter bandwidth is 1.1 MHz. The amplitude of the signal after balanced

photodetection, $V_{pd}(t)$, is plotted as a function of the loop gain. Experimental and simulation results show that as the loop gain is increased, the amplitude of $V_{pd}(t)$ is reduced, i.e. the linearity of the demodulator is improved. Good agreement between the experimental and simulation results is obtained for one tone measurement.

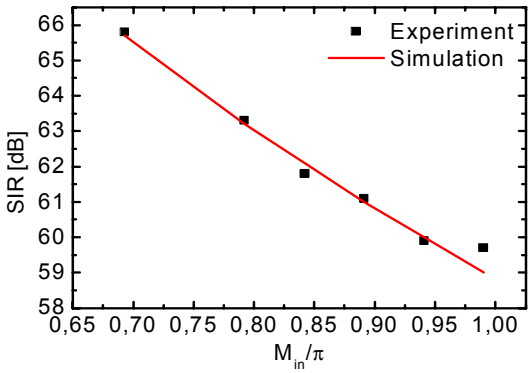

Fig. 3. Two tone measurement. SIR as a function of input signal modulation depth.

In Fig. 3, results of the two tone measurement are shown together with the simulation results. The SIR is plotted as a function of the modulation depth, M_{in}, of the input RF signal. The input RF signal frequencies are: f^s_1=150 kHz and f^s_2=170 kHz. As expected, the SIR decreases as M_{in} is increased. Once again good agreement between the model and experimental results is observed.

IV. Sampling Loop Simulation Results

In this section, the linearity of the optical phase demodulator, based on sampling phase-locked loop, is investigated by computing the SIR of the demodulated signal. The intermodulation is the magnitude of the mixing terms: $\{2(\omega_1-\omega_{ls}) - (\omega_2-\omega_{ls}), 2(\omega_2-\omega_{ls}) - (\omega_1-\omega_{ls})\}$. An RF input signal modulation depth of $\pi/2$ is assumed in all simulation results. In Fig. 4, the SIR is computed as a function of the Full-Width-Half-Maximum (FWHM) of the pulsed optical source signal for selected values of the loop gain. The input RF signal frequencies are ω_1=20GHz + 0.9GHz, ω_1=20GHz + 1.6GHz and ω_{ls}=20GHz. The downconverted IF components, at which the loop will operate, are: $\omega_{IF,1} = \omega_1-\omega_{ls}$ and $\omega_{IF,2} = \omega_2-\omega_{ls}$. The constant lines correspond to the SIR obtained by the baseband loop for the corresponding values of the loop gain. For the baseband case ω_1=0.9 GHz and ω_2=1.6 GHz. In general, Fig. 4 shows that the SIR decreases as the FWHM is increased. This is in accordance with (3) and indicates that the sampling induces a penalty in the SIR. However, it should be noted that for the open-loop sampling system there is no degradation in the SIR as the pulse width is varied. Furthermore, we observe from Fig.4 that as the pulse width (FWHM) is decreased, the SIR of the sampling loop approaches the value obtained by the baseband loop.

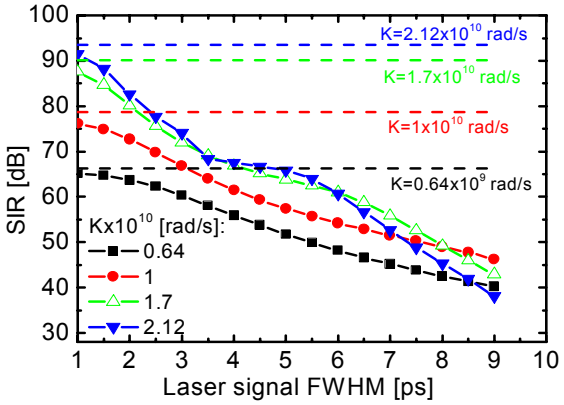

Fig. 4. SIR as a function of FWHM of the laser signal for selected values of the loop gain.

However, very short pulses (~1ps) are required in order to preserve the SIR. Fig. 4 furthermore indicates that for relatively high values of the FWHM, increasing K does not improve the SIR. We therefore need to investigate how the SIR of the demodulated signal is affected by increasing the loop gain.

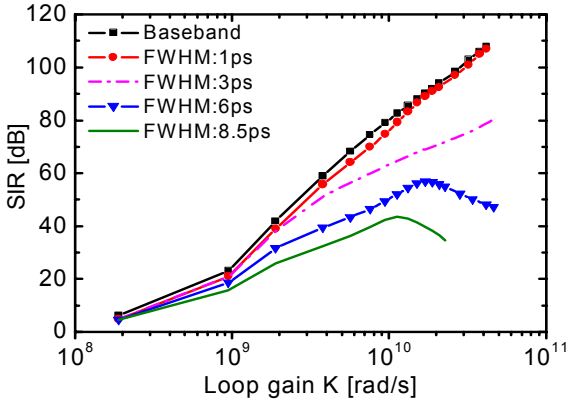

Fig. 5. SIR as a function of loop gain, K, for selected values of the FWHM of the pulsed laser source.

In Fig. 5, the SIR is computed as a function of the loop gain for different values of the FWHM. As a reference, we also plot the SIR obtained by the baseband loop in the same figure. Fig. 5 shows that for increasing loop gain and pulse width (FWHM), the SIR of the demodulated signal, obtained by the sampling loop deviates from the SIR obtained by the baseband loop. The penalty in the SIR is increased as the loop gain is increased. This is in accordance with (3), as discussed earlier. Fig. 5 also shows that the SIR is less sensitive to the FWHM for low values of the loop gain. Furthermore, the SIR curve starts to decrease, for the FWHM of 6 ps and 8.5 ps, as the loop gain is sufficiently increased. The value of the loop gain for which the SIR starts to decrease, decreases with increasing pulse width

(FWHM). For the FWHM of 1 ps and 3 ps, a decrease in the SIR is not observed in the considered range (obtainable in practice) of the loop gain. For the FWHM of 8.5 ps pulse width, the loop looses its lock if the loop gain is increased beyond 2.5×10^{10} rad/s.

Next, it is investigated how SIR is affected by input RF signal frequency (Fig. 6).The FWHM is set to 1 ps.

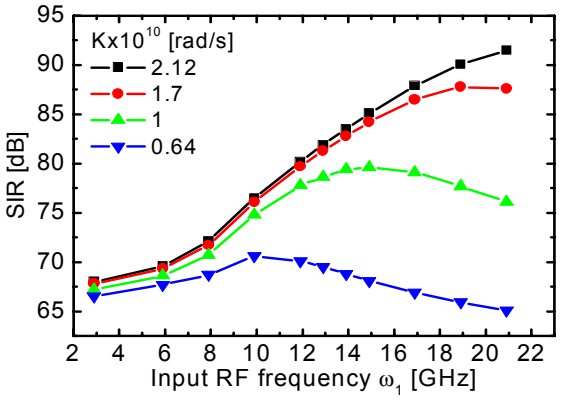

Fig. 6. SIR as a function of input signal frequency for selected values of the loop gain. FWHM of the laser signal: 1 ps.

The frequency difference $\omega_1 - \omega_{ls}$ and $\omega_2 - \omega_{ls}$ is held constant and the sampling loop will therefore operate at a constant intermediate frequency. Fig. 6 indicates that for relatively high values of loop gain: 2.12×10^{10} and 1.17×10^{10} rad/s, the SIR of the demodulated signal increases as the input signal frequency is increased. For relatively low values of the input RF signal frequency, the dependence of the SIR on the loop gain is negligible. In that case the SIR is limited by the nonlinearities of the low-frequency optical pulsed source. For the relatively low value of the loop gain, ($K=0.64 \times 10^{10}$ rad/s), the SIR does not seem to be much affected by increasing ω_1. Furthermore, for $K=0.64 \times 10^{10}$ and 1×10^{10}rad/s, there is an optimal value of the input signal frequency for which the SIR is increased.

So far, the effect of the finite delay in the loop has been considered to be small. In a baseband loop, the effect of loop delay is well known to limit the available loop gain, while maintaining stability [5]. The delay gets more significant the higher the frequency. In a sampled loop, the effective feedback delay is given by that of the pulse rate. No information can in this case be forwarded when no pulse is present in the loop, assuming the pulse width is narrower than the physical delay of the loop. In other words; the sampled loop will operate more efficiently at higher input frequencies. Fig. 7 shows the effect of a physical loop delay in a sampled loop. A 20 GHz pulse rate, 1 GHz IF and 0.5 rad modulation depth in a second order loop has been assumed. Further, idealized delta pulses have been assumed to clearly isolate the impact of the loop delay. The performance degrades slowly with increasing delay up to the point where the delay exceeds the pulse repetition ratio, after which step degradation in performance occurs corresponding to a delayed feedback to the second proceeding pulse.

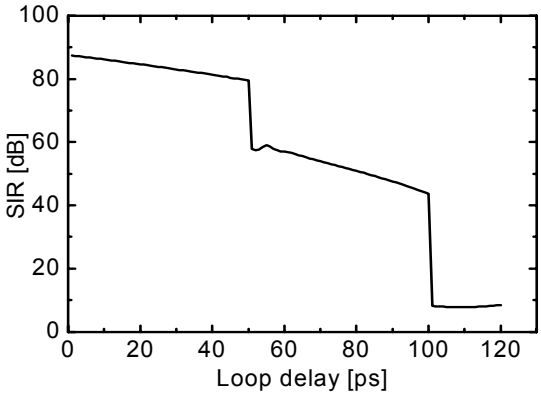

Fig. 7. SIR as a function of loop delay in a sampled second order feedback loop with 20 GHz pulse rate and 1 GHz IF.

It can be observed that the effect of loop delay is relatively weak compared to the pulse rate.

VII. Conclusion

A novel approach of using optical sampling, in order to increase operation frequency of the optical phase demodulator, has been theoretically investigated. The optical sampling inherently induces a penalty in the SIR compared to the baseband loop. However, for very short pulse widths (<2 ps) and high input signal frequencies, the penalty is very small making this technique promising for high-frequency analog optical links.

Acknowledgement

The authors thank Larry Coldren, Larry Lembo, Steve Pappert, and Roy Smith for useful conversations and input. This work was supported by DARPA under the PHOR-FRONT program.

References

[1] C.H. Cox III et al.,"Limits on the Performance of RF-Over-Fiber Links and Their Impact on Device Design," IEEE Trans. on Microwave Theory and Tech., vol. 54, no. 2, pp. 906-920, Feb. 2006.

[2] R.F. Kalman et al.,,"Dynamic range of coherent analog fiber-optic links," Journal of Lightwave Techn., vol. 12, no. 7, pp. 1263-1277, July 1994.

[3] H. F. Chou, et al, "SFDR Improvement of a Coherent Receiver Using Feedback", in Proc. of IEEE Conference on Coherent Optical Technologies and Applications (COTA), paper CFA3, 2006

[4] D. Zibar, et al., "Time Domain Analysis of a Novel Phase-Locked Coherent Optical Demodulator", in Proc. of IEEE Conference on Coherent Optical Technologies and Applications (COTA) paper JWB1, 2006

[5] F. Gardner, "Phase-lock techniques," 3rd edition, John Wiley and Sons, 2004.